Letter

Laser-driven time-limited light-sail acceleration of protons for tumor radiotherapy

Y. F. Li,[1,*] X. F. Shen,[2,*] Y. L. Yao,[1] S. Z. Wu,[3] A. Pukhov,[2] and B. Qiao[1,4,5,†]

[1]*Center for Applied Physics and Technology, HEDPS and SKLNP, School of Physics, Peking University, Beijing 100871, China*
[2]*Institut für Theoretische Physik I, Heinrich-Heine-Universität Düsseldorf, 40225 Düsseldorf, Germany*
[3]*Center for Advanced Material Diagnostic Technology, Shenzhen Technology University, Shenzhen 518118, China*
[4]*Collaborative Innovation Center of IFSA (CICIFSA), Shanghai Jiao Tong University, Shanghai 200240, China*
[5]*Frontiers Science Center for Nano-optoelectronic, Peking University, Beijing 100094, China*

(Received 3 September 2022; revised 28 December 2022; accepted 24 February 2023; published 20 March 2023)

A laser-driven time-limited light-sail acceleration scheme for proton tumor radiotherapy is proposed, where a whole spread-out Bragg peak (SOBP) dose delivery to the tumor region can be achieved with a single laser shot. By using a proper match of laser and ultrathin foil target parameters, proton light-sail acceleration terminates immaturely before the transverse instability grows up, resulting in the production of a proton beam with the required highly peaked energy spectrum and sufficiently large particle number. A self-consistent combination of three-dimensional particle-in-cell simulations and GEANT4 microdosimetry simulations in a water phantom model demonstrates that our scheme is able to deliver a single-shot SOBP dose up to 1.76 Gy to cubic-centimeter-scale volumes on a nanosecond timescale for shallow-seated tumors and around 0.56 Gy for deep-seated tumors, where the deviations of dose equivalent in the flat SOBP region are both within the clinically acceptable range.

DOI: 10.1103/PhysRevResearch.5.L012038

Radiation therapy, also called radiotherapy (RT), is a major cancer treatment method that uses high doses of radiation to kill cancer cells. Proton RT is thought to be more advantageous than commonly used photon RT [1,2], because the proton beam releases massive energy at a desired depth decided by the beam energy, but only a small amount of the dose is released along the beam path. These characteristics are well known as the "Bragg peak" [3]. Through these characteristics, the proton beam not only precisely irradiates the tumor, but also minimizes harm to the surrounding normal tissues. However, due to high cost and the large size of conventional accelerators [4], only a small number of proton RT facilities are in use worldwide. In this perspective, laser-driven proton acceleration (LDPA) offers a potentially more compact and cost-effective means of delivering proton beams for RT. On the other hand, the proton beams delivered from laser-driven accelerators are generally of an ultrashort duration, resulting in radiobiological dose deposition at an ultrahigh dose rate, many orders of magnitude higher than those from conventional accelerators. This brings another beneficial FLASH RT effect [5–10] that reduces radiation-induced damage in healthy tissue without decreasing antitumor effectiveness.

Significant effort is ongoing to demonstrate the laser-accelerated proton beam qualities required to make the above proposition viable [11–19]. Remarkable advances have been seen recently with a substantial proton energy increase in experiments, when nanometer-scale ultrathin foil targets and high-contrast intense lasers are applied. Now, proton beams with the maximum energy close to 100 MeV can be robustly obtained [16,18], high enough for the therapy of several shallow-seated tumors [1,20].

On the other hand, the clinical proton RT requires delivery of a constant dose throughout the depth extent of the tumor while minimizing the dose deposited behind its distal edge, termed as a spread-out Bragg peak (SOBP) dose distribution [21–23]. In contrast to conventional accelerator-based proton RT, where monoenergetic pencil beams are produced and the SOBP is achieved by scanning the complete depth of the tumor with a weighted superposition of beams at a broad energy window [24–26], laser-accelerated proton beams are generally far from monoenergetic, but with a high charge. As a consequence, if using a conventional energy selection and scanning system [25], the particle loss is unacceptable. Note that the broad energy spectrum from LDPA may already contain the required energy window for SOBP with sufficient amounts of protons to deliver enough of a dose for treatment over a few or even a single laser shot. Therefore, a critical challenge that LDPA needs to overcome before its application in clinical RT is how to produce a proton beam with a proper energy spectrum so that a uniform SOBP dose delivery to the whole tumor region can be achieved.

In this Letter, we propose a scheme named time-limited "light-sail" (LS) acceleration, as shown in Fig. 1(a), for laser-driven proton RT, where the proton beam with the required asymmetric energy spectrum (with a sharp distal falloff at the high-energy range) can be obtained so that a whole SOBP dose delivery to the tumor region is achieved

*These authors contributed equally to this work.
†Corresponding author: bqiao@pku.edu.cn

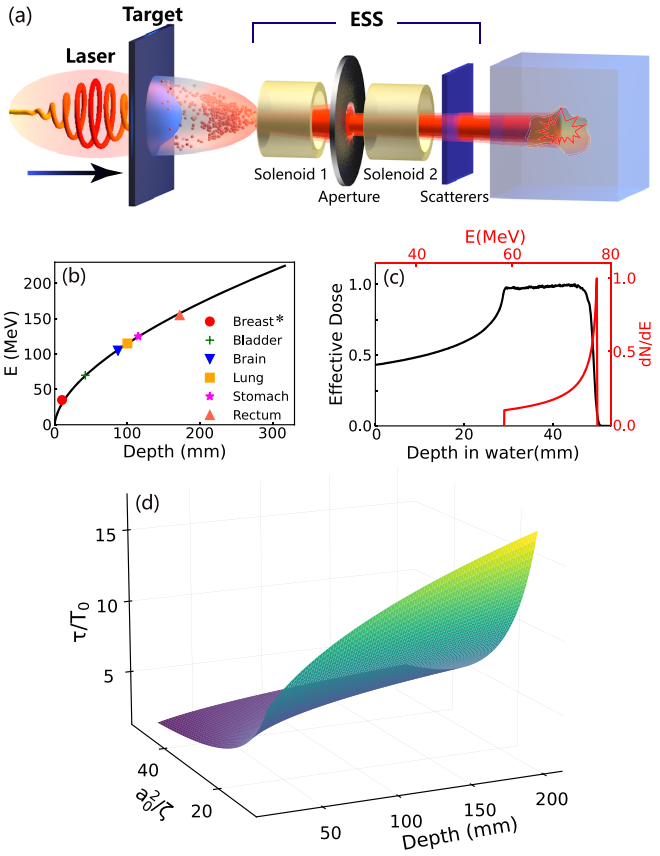

FIG. 1. (a) Schematic of laser-driven proton RT. Quasimonoenergetic protons accelerated from nm-thin foils enter the water phantom after being selected by an energy selecting system (ESS). (b) Required peak energies $E_{\rm peak}$ for treatment of cancers at different depths [4,20]. (c) shows the ideal proton spectrum (red line) and the corresponding SOBP dose distribution (black line). (d) Maximum laser pulse duration τ_L for different treatment depths and a_0^2/ζ.

with a single laser shot. In this scheme, under a proper match between the target and laser parameters, the time for proton LS acceleration is limited so that it terminates before the transverse instability starts to grow rapidly. Therefore, the electron heating and the energy spectral broadening induced by hot electrons can be significantly suppressed. These together lead to a suitable proton spectrum that can be used to create a flat SOBP. A self-consistent combination of three-dimensional (3D) particle-in-cell (PIC) simulations and GEANT4 microdosimetry simulations in a water phantom model demonstrates that protons accelerated by petawatt femtosecond laser pulses are able to deliver a single-shot SOBP dose up to 1.76 Gy to cubic-centimeter-scale volumes on a nanosecond timescale for shallow-seated tumors, where the deviations of dose equivalent in the SOBP region are within the clinical acceptable range.

First, we consider a broad energy spectrum generally obtained in LDPA. Based on the solution to the Boltzmann kinetic equation for a proton distribution function, the exact proton spectrum needed to achieve a SOBP dose delivery within a depth interval $d_{\rm min} < d < d_{\rm max}$ is determined as [27]

$$f(\tilde{E}) = H(\tilde{E} - \tilde{E}_{\rm min})H(\tilde{E}_{\rm max} - \tilde{E})\frac{\tilde{E}}{\left(\tilde{E}_{\rm max}^2 - \tilde{E}^2\right)^{0.57}}, \quad (1)$$

where $H(x)$ is the unit-step function, $\tilde{E} = E/m_pc^2$ is the normalized proton energy, $\tilde{E}_{\rm min,max} = (\eta d_{\rm min,max})^{1/1.715}$ with $\eta = 15n_e/(m_ec^2)e^4/(4\pi\varepsilon_0^2 m_pc^2)$, and n_e the electron density. According to Eq. (1), we calculate the required proton energies for the most common tumors [4,20] [see the different colored markers in Fig. 1(b)]. As an example, in Fig. 1(c), we correspondingly show the ideal proton energy spectrum given by Eq. (1) (red line) for the therapy of shallow-seated tumors and the obtained SOBP dose distribution (black). It is evident that the energy spectrum is characterized by an asymmetric profile with a slow rise and sharp distal falloff in energy. In other words, $E_{\rm max} \simeq E_{\rm peak}$ is optimal to achieve a flat SOBP.

Second, among various LDPA mechanisms [28,29], one promising option to obtain quasimonoenergetic proton beams is to push a nanometer-scale foil target directly by laser radiation pressure, known as the LS acceleration [30–33]. Ideally, the peak energy is described by the LS model [32,34],

$$E_{\rm peak} = \frac{\xi^2}{2(1+\xi)}m_pc^2, \quad (2)$$

where $\xi = 2\pi(Z/A)(m_e/m_p)(a_0^2\tau_L/\zeta)$, Z/A is the charge to mass ratio, a_0 is the normalized laser intensity, τ_L is the normalized pulse duration, and $\zeta = \pi(n_e/n_c)(l/\lambda)$. Here, n_c, l, and λ correspond to the critical density, initial target thickness, and laser wavelength, respectively.

However, in realistic situations, detrimental transverse instabilities such as a Rayleigh-Taylor-like instability (RTI) inevitably develop [35,36], and the accelerating foil becomes severely deformed. A significant number of hot electrons are produced, forming a moving hot electron cloud around the accelerating foil. The additional acceleration of protons by these moving hot electrons, where the mechanism is similar to the target normal sheath acceleration in a moving reference frame [34,37,38], has to be taken into account and results in strong broadening of the energy spectrum, far from that of Eq. (1).

Various methods have been proposed to stabilize the LS acceleration such as via suppressing the development of the transverse instability [33,35,36] and considering the dynamic ionization of a high-Z coating in front of a thin foil [14]. The latter was demonstrated by recent experiment [39]. Here, different from previous works which aimed to enhance the peak energy or achieve quasimonoenergetic ion beams, we focus on optimizing the obtained proton energy spectrum to make it feasible for single-shot cancer therapy. To realize this, we propose a scheme, named time-limited LS acceleration, where the time for proton LS acceleration is limited so that it terminates before the transverse instability starts to grow rapidly. The upper limit of the pulse duration is determined by the growth rate of transverse instability

$$\tau_L[T_0] \leqslant \tau_{\rm RT} \simeq 136a_0^{-1}\left(\sqrt{\frac{2}{\kappa}}l[\mu{\rm m}]\lambda[\mu{\rm m}]\sqrt{\frac{n_e}{n_c}}\right)^{1/2}, \quad (3)$$

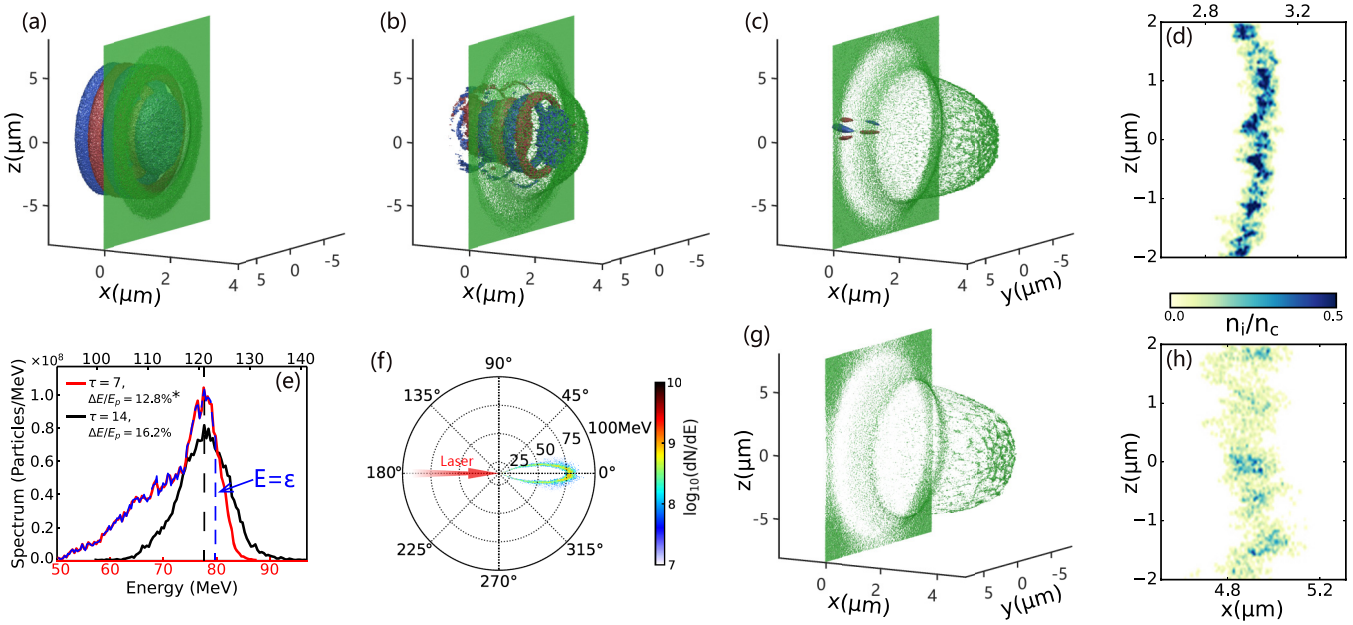

FIG. 2. Isosurface of proton density and laser field E_y at (a) $t = 7T_0$, (b) $12T_0$, and (c) $18T_0$ for the case with $\tau_L = 7$. (e) The final energy spectrum of protons within 10° for the cases with $\tau_L = 7$ (red) and $\tau_L = 14$ (black). (f) Angular distribution of protons at $t = 18T_0$ for the case with $\tau_L = 7$. (g) Proton distribution at $t = 25T_0$ for $\tau_L = 14$. (d) and (h) show the longitudinal cuts (at $y = 0$) of the proton density distribution in (c) and (g), respectively.

where τ_{RT} is the growth time of RTI [40], $\kappa = (2c^2 - v_{\mathrm{osc}}^2)/2\gamma_0 c^2$, and v_{osc} is the electron quiver velocity. Furthermore, by using a circularly polarized laser pulse, not only the oscillating component of the $j \times B$ vanishes, but also the Rayleigh-Taylor-like instability does not have time to develop to the nonlinear stage. Therefore, the additional acceleration caused by electron heating could be greatly suppressed and the monoenergetic feature can survive especially the sharp distal falloff feature in energy, i.e., a preferred spectrum with $E_{\mathrm{peak}} \simeq E_{\mathrm{max}}$ can be obtained. By considering Eqs. (2) and (3), the required τ_L and a_0^2/ζ for different treatment depths can be easily determined [see Fig. 1(d)]. This is important for the parameter design and experimentation of future laser facilities towards the treatment of various tumors.

In order to demonstrate the feasibility of our scheme, we first conduct 3D PIC simulations with the EPOCH code [41]. To achieve a proper proton beam for the treatment of shallow-seated tumors, based on Eqs. (2) and (3), we consider a laser pulse with $a_0 = 38$, $\tau_L = 7$, and $\lambda = 800$ nm. The transverse profile is fourth-order super-Gaussian with radius $r = 5$ μm to save computational resources, while the temporal is Gaussian. The main target is composed of fully ionized aluminum ions with $n_e = 200n_c$ and thickness 40 nm. At the rear surface, we put a carbon-hydrogen layer to mimic contaminants. Its thickness is 8 nm and the number density ratio of the proton to carbon ion is H : C = 1 : 9. Substituting the above parameters into Eq. (3) yields $\tau_{\mathrm{RT}} \approx 8.5$, and therefore, to confirm the effect of pulse duration, a simulation with $\tau_L = 14$ and other parameters remaining unchanged is performed. The simulation box is 12 μm × 16 μm × 16 μm in the (x, y, z) directions, respectively.

Figures 2(a)–2(c) show the laser field E_y and proton density distribution at $t = 7T_0$, $12T_0$, and $18T_0$, respectively. One can see that protons are stably pushed forward by light pressure, while the target remains opaque throughout the acceleration. This is because the pulse duration is relatively short and the transverse instability is significantly suppressed [comparing Figs. 2(d) and 2(h)] since it does not have a sufficient time to reach the nonlinear stage. The final proton beam is well collimated [Fig. 2(f)]and the energy spectrum of protons within 10° is quasimonoenergetic with a peak energy 77.8 MeV, energy spread 10%, and more importantly, a relatively sharp distal falloff with $\Delta E = E_{\mathrm{max}} - E_{\mathrm{peak}} \approx 10$ MeV [red line in Fig. 2(e)]. There are about 10^9 protons within full width at half maximum. Though this spectrum is not exactly the same as the profile defined by Eq. (1), it has the key asymmetric feature which ensures the production of a flat SOBP dose distribution. Note that protons at the laser wing side region inevitably undergo transverse thermal expansion simultaneously during their LS acceleration [29,42,43], because the accelerating target deforms and electron heating occurs at a later stage due to the transversely nonuniform laser intensity distribution. This leads to the protons having larger divergences when they are accelerated to higher energies. On the other hand, protons near the laser axis undergo a stable radiation pressure acceleration (RPA) with no expansion, achieving high energies with small divergences. Combining these two groups of protons and further noting that the laser intensity at the wing side is always comparatively lower, the divergence of the proton beam has the feature of peaking at moderate energies, shown in Fig. 2(f), which is inherently different from that in the target normal sheath acceleration [44,45].

For the therapy of cubic-centimeter-scale shallow-seated tumors [46,47], we select protons within 10° [in experiment this can be easily accomplished only via an aperture; see the

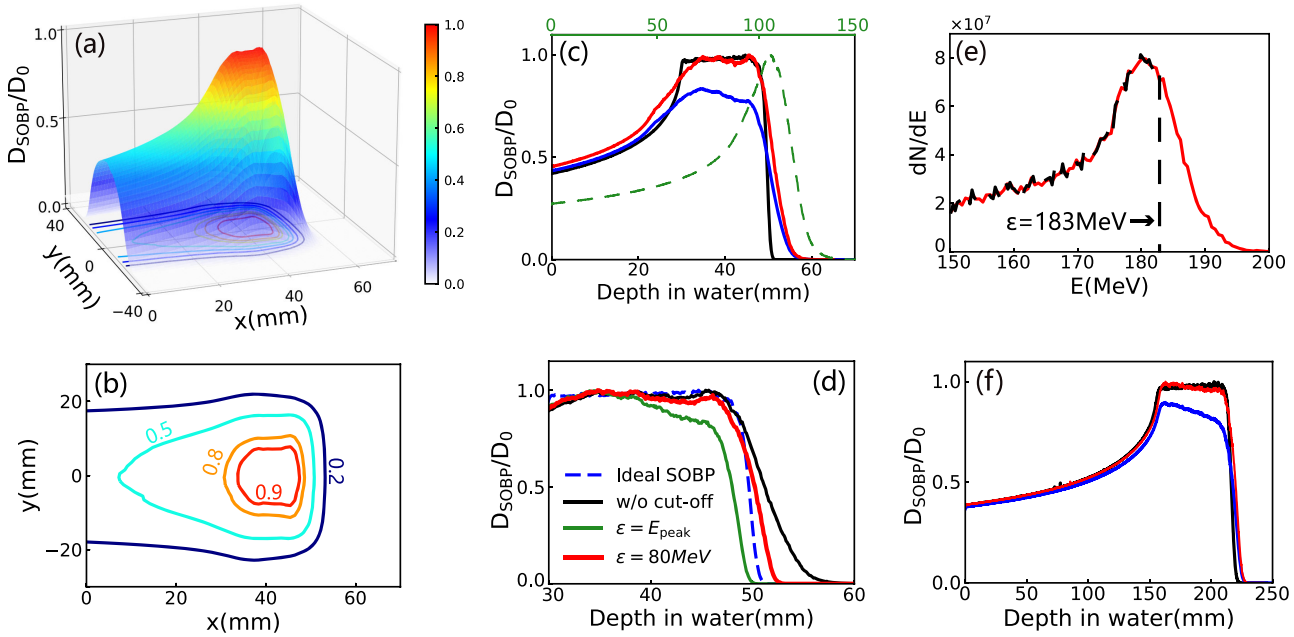

FIG. 3. (a) 3D distribution of a normalized proton dose for the treatment of shallow-seated tumors, and its projection on the (x, y) plane (b). (c) Lineout of the physical dose curve (blue), effective dose curve (red), and ideal SOBP curve (black) along the x direction. In comparison, the green dashed lines show the effective dose curve from the case with $\tau_L = 14$. (d) Comparison of the effective dose curves obtained from different cases. (e) The obtained proton spectrum for deep-seated tumors, where the black dashed line shows the spectrum by filtering out protons with energy $>$ 183 MeV. (f) correspondingly shows a lineout of the physical dose curve (blue), effective dose curve (red), and ideal SOBP curve (black) along the x direction.

schematic Fig. 1(a)], and substitute their data [i.e., momentum (p_x, p_y, p_z) and energy E] into GEANT4 [48] by the probability sampling method to obtain the proton dose distribution. In GEANT4, the inelastic scattering and nuclear reaction are self-consistently considered. Note that in principle, the complete ESS (specifically the solenoids) is not necessary for our scheme since we only select protons within a certain angle. However, for more realistic irregular tumors, one may need the complete ESS to manipulate the proton beams precisely to conform to the specific shape of the tumors.

Figure 3 shows the results of the proton energy deposition in water. In Fig. 3(a), one can clearly see a rather flat spread peak in the 3D dose distribution, corresponding to the SOBP region. Its extent in depth, defined as the distance between the distal and proximal 90% points of the peak dose [49], is located at 30–48 mm in the x direction [red line in Fig. 3(c)], and in the y and z directions [Fig. 3(b)], it is within -10 to 10 mm. In this region, the effective dose is about 1.76 GyE, comparable to the dose requirement ($\sim$2 Gy/fraction) for the therapy of shallow-seated tumors. Therefore, it is promising to achieve a whole SOBP dose delivery to the tumor region with a single laser shot. Further, we evaluate the obtained dose compliance. Within the SOBP, the deviation of the dose equivalent δ varies from -2.98% to 2.35% and the normalized standard deviation of the dose equivalent $\sigma = D_{\mathrm{STDEV}}/D_{\mathrm{mean}} = 2.31\%$, where D_{mean} is the average dose and D_{STDEV} is the standard deviation. This indicates that the obtained dose uniformity is within the requirements of clinical RT. Moreover, compared to the ideal SOBP [black line in Fig. 3(c)] simulated from the spectrum given by Eq. (1), one can see that the differences are minor except a slightly wider distal falloff width w_d (about 4.3 mm), defined as the width of distal dose falloff from 80% to 20% points of the peak dose [49]. The detailed comparisons are shown in Table I. Notice that compared to the other known regimes, our scheme does not require the sophisticated ESS (especially the solenoids) to generate the pencil-like proton beams and therefore can avoid the huge particle loss. Moreover, the protons of interest here are those with energies close to the cutoff energy instead of the low-energy ones. This determines that to treat tumors at the same depth, the required laser power (or intensity) in our scheme can be much lower.

During the proton transport, the proton bunch duration spreads in time to about 0.35 ns, leading to an instantaneous dose rate (IDR) high up to 5.0×10^9 Gy/s, several orders of magnitude higher than that from conventional accelerators. Such a high dose rate is important for the investigation of the FLASH RT effect. In addition, to further reduce the w_d, an ESS [see Fig. 1(a)] can be used to optimize the energy spectrum [10,50]. For example, by filtering out protons with energy $>$80 MeV [blue dashed line in Fig. 2(e)], the obtained

TABLE I. Properties of the SOBP dose distribution in Fig. 3(d).

	w_{SOBP} (mm)	w_d (mm)	δ	σ
Ideal SOBP	29.6–48.3	1.0	-3.24% to 2.11%	1.73%
Without cutoff	30.1–47.9	4.3	-2.98% to 2.35%	2.31%
$\varepsilon = 80$ MeV	29.7–47.4	2.7	-3.77% to 3.37%	2.48%

SOBP dose distribution [red line in Fig. 3(d)] is very close to the ideal one (black dashed). This also demonstrates that our results are not sensitive to the potential small fluctuations existing in proton beams.

In comparison, for the case with $\tau_L = 14$, induced by the nonlinear development of the transverse instability [Fig. 2(h)] and severe electron heating, the obtained proton energy spectrum is significantly broadened [black line in Fig. 2(e)] with $\Delta E \approx 20$ MeV. The spectrum shows an almost symmetric distribution, instead of an asymmetric one required for producing a flat SOBP. Therefore, the obtained proton dose distribution no longer shows a flat SOBP dose distribution [see the green dashed line in Fig. 3(c)]. This demonstrates the importance of the time-limited LS acceleration in obtaining suitable energy spectra towards laser-driven proton RT.

For the treatment of deep-seated tumors such as lung cancer, the required proton peak energy is about 180 MeV [51]. According to Eqs. (2) and (3), we further perform a 3D simulation where a laser pulse with $a_0 = 66$ and $\tau_L = 7$ is used and the target parameters are correspondingly set as $n_e = 300 n_c$, $d_1 = 48$ nm, and $d_2 = 8$ nm.

Figure 3(e) shows the obtained proton energy spectrum (red line) which is peaked at about 180 MeV and has an energy spread of about 8%. By substituting the obtained proton data into GEANT4, we observe a flat SOBP dose distribution [red line in Fig. 3(f)] locating at 160–210 mm in the x direction and -18 to 18 mm in the transverse directions. The effective dose is 0.56 GyE with δ from -1.81% to 6.75%, $\sigma = 1.86\%$, and $w_d = 8.0$ mm. The IDR is about 2.4×10^9 Gy/s. Note that here to optimize the dose distribution, we filter out protons with energy >183 MeV [black dashed line in Fig. 3(e)]. Moreover, the treatment of deep-seated tumors requires a higher dose of about 5 Gy/fraction [51], which means at least 9 proton beams are required in a single treatment. Considering that a reasonable treatment time is around 1 min [52], the laser repetition rate should be about 0.15 Hz, which can be easily achieved with state-of-the-art PW laser facilities [53].

In conclusion, a scheme for generating monoenergetic proton beams with a sharp distal falloff energy spectrum suitable for laser-driven proton RT has been proposed, where time-limited LS acceleration is achieved by properly matching the laser and target parameters. A systematic study self-consistently combining 3D PIC and GEANT4 simulations was performed to show that a single-shot proton beam can deliver a flat SOBP distribution with dose up to Gy, where the dose uniformity is within the requirements of clinical treatment.

This work is supported by the National Key R&D Program of China, Grants No. 2022YFA1603200 and No. 2022YFA1603201; National Natural Science Foundation of China, Grants No. 12135001, No. 11921006, and No. 11825502; Strategic Priority Research Program of CAS, Grant No. XDA25050900. BQ acknowledges support from the National Natural Science Funds for Distinguished Young Scholar, Grant No. 11825502. The simulations are carried out on the Tianhe-2 supercomputer at the National Supercomputer Center in Guangzhou.

[1] K. W. D. Ledingham, P. R. Bolton, N. Shikazono, and C.-M. Ma, Towards laser driven hadron cancer radiotherapy: A review of progress, Appl. Sci. **4**, 402 (2014).

[2] S. V. Bulanov and V. S. Khoroshkov, Feasibility of using laser ion accelerators in proton therapy, Plasma Phys. Rep. **28**, 453 (2002).

[3] R. R. Wilson, Radiological use of fast protons, Radiology **47**, 487 (1946).

[4] D. Schulz-Ertner and H. Tsujii, Particle radiation therapy using proton and heavier ion beams, J. Clin. Oncol. **25**, 953 (2007).

[5] M. Durante, E. Bräuer-Krisch, and M. Hill, Faster and safer? FLASH ultra-high dose rate in radiotherapy, Brit. J. Radiol. **91**, 20170628 (2017).

[6] M.-C. Vozenin, J. H. Hendry, and C. L. Limoli, Biological benefits of ultra-high dose rate FLASH radiotherapy: Sleeping Beauty awoken, Clin. Oncol. **31**, 407 (2019).

[7] J. D. Wilson, E. M. Hammond, G. S. Higgins, and K. Petersson, Ultra-high dose rate (FLASH) radiotherapy: Silver bullet or fool's gold? Front. Oncol. **9**, 1563 (2020).

[8] P. Chaudhary, G. Milluzzo, H. Ahmed, B. Odlozilik, A. McMurray, K. M. Prise, and M. Borghesi, Radiobiology experiments with ultra-high dose rate laser-driven protons: Methodology and state-of-the-art, Front. Phys. **9**, 624963 (2021).

[9] J. Ehlert, M. Piel, F. Boege, M. Cerchez, R. Haas, G. E. Iliakis, R. Prasad, O. Willi, and C. Monzel, An experimental platform for studying the radiation effects of laser accelerated protons on mammalian cells, AIP Adv. **11**, 065208 (2021).

[10] F. Kroll, F.-E. Brack, C. Bernert, S. Bock, E. Bodenstein, K. Brüchner, T. E. Cowan, L. Gaus, R. Gebhardt, U. Helbig *et al.*, Tumour irradiation in mice with a laser-accelerated proton beam, Nat. Phys. **18**, 316 (2022).

[11] H. Schwoerer, S. Pfotenhauer, O. Jäckel, K.-U. Amthor, B. Liesfeld, W. Ziegler, R. Sauerbrey, K. W. D. Ledingham and T. Esirkepov, Laser-plasma acceleration of quasi-monoenergetic protons from microstructured targets, Nature (London) **439**, 445 (2006).

[12] S. Kar, H. Ahmed, R. Prasad, M. Cerchez, S. Brauckmann, B. Aurand, G. Cantono, P. Hadjisolomou, C. L. S. Lewis, A. Macchi *et al.*, Guided post-acceleration of laser-driven ions by a miniature modular structure, Nat. Commun. **7**, 10792 (2016).

[13] F. Wagner, O. Deppert, C. Brabetz, P. Fiala, A. Kleinschmidt, P. Poth, V. A. Schanz, A. Tebartz, B. Zielbauer, M. Roth *et al.*, Maximum Proton Energy above 85 MeV from the Relativistic Interaction of Laser Pulses with Micrometer Thick CH_2 Targets, Phys. Rev. Lett. **116**, 205002 (2016).

[14] X. F. Shen, B. Qiao, H. Zhang, S. Kar, C. T. Zhou, H. X. Chang, M. Borghesi, and X. T. He, Achieving Stable Radiation Pressure Acceleration of Heavy Ions via Successive Electron Replenishment from Ionization of a High-Z Material Coating, Phys. Rev. Lett. **118**, 204802 (2017).

[15] M. Nakatsutsumi, Y. Sentoku, A. Korzhimanov, S. N. Chen, S. Buffechoux, A. Kon, B. Atherton, P. Audebert, M. Geissel,

L. Hurd *et al.*, Self-generated surface magnetic fields inhibit laser-driven sheath acceleration of high-energy protons, Nat. Commun. **9**, 280 (2018).

[16] A. Higginson, R. J. Gray, M. King, R. J. Dance, S. D. R. Williamson, N. M. H. Butler, R. Wilson, R. Capdessus, C. Armstrong, J. S. Green *et al.*, Near-100 MeV protons via a laser-driven transparency-enhanced hybrid acceleration scheme, Nat. Commun. **9**, 724 (2018).

[17] R. Matsui, Y. Fukuda, and Y. Kishimoto, Quasimonoenergetic Proton Bunch Acceleration Driven by Hemispherically Converging Collisionless Shock in a Hydrogen Cluster Coupled with Relativistically Induced Transparency, Phys. Rev. Lett. **122**, 014804 (2019).

[18] T. P. Frazer, R. Wilson, M. King, N. M. H. Butler, D. C. Carroll, M. J. Duff, A. Higginson, J. Jarrett, Z. E. Davidson, C. Armstrong, H. Liu, D. Neely, R. J. Gray, and P. McKenna, Enhanced laser intensity and ion acceleration due to self-focusing in relativistically transparent ultrathin targets, Phys. Rev. Res. **2**, 042015(R) (2020).

[19] X. F. Shen, A. Pukhov, and B. Qiao, Monoenergetic High-Energy Ion Source via Femtosecond Laser Interacting with a Microtape, Phys. Rev. X **11**, 041002 (2021).

[20] J. Fontenot, P. Taddei, Y. Zheng, D. Mirkovic, T. Jordan, and W. Newhauser, Equivalent dose and effective dose from stray radiation during passively scattered proton radiotherapy for prostate cancer, Phys. Med. Biol. **53**, 1677 (2008).

[21] A. M. Koehler and W. M. Preston, Protons in radiation therapy, Radiology **104**, 191 (1972).

[22] T. Bortfeld and W. Schlegel, An analytical approximation of depth-dose distributions for therapeutic proton beams, Phys. Med. Biol. **41**, 1331 (1996).

[23] T. Kanai, Y. Furusawa, K. Fukutsu, H. Itsukaichi, K. Eguchi-Kasai, and H. Ohara, Irradiation of mixed beam and design of spread-out Bragg peak for heavy-ion radiotherapy, Radiat. Res. **147**, 78 (1997).

[24] A. M. Koehler, R. J. Schneider, and J. M. Sisterson, Range modulators for protons and heavy ions, Nucl. Instrum. Methods **131**, 437 (1975).

[25] T. Nakagawa and K. Yoda, A method for achieving variable widths of the spread-out Bragg peak using a ridge filter, Med. Phys. **27**, 712 (2000).

[26] D. Jette and W. Chen, Creating a spread-out Bragg peak in proton beams, Phys. Med. Biol. **56**, N131 (2011).

[27] E. Fourkal, I. Velchev, J. Fan, W. Luo, and C.-M. Ma, Energy optimization procedure for treatment planning with laser-accelerated protons, Med. Phys. **34**, 577 (2007).

[28] A. Macchi, M. Borghesi, and M. Passoni, Ion acceleration by superintense laser-plasma interaction, Rev. Mod. Phys. **85**, 751 (2013).

[29] B. Qiao, X. F. Shen, H. He, Y. Xie, H. Zhang, C. T. Zhou, S. P. Zhu and X. T. He, Revisit on ion acceleration mechanisms in solid targets driven by intense laser pulses, Plasma Phys. Controlled Fusion **61**, 014039 (2019).

[30] T. Esirkepov, M. Borghesi, S. V. Bulanov, G. Mourou, and T. Tajima, Highly Efficient Relativistic-Ion Generation in the Laser-Piston Regime, Phys. Rev. Lett. **92**, 175003 (2004).

[31] B. Qiao, M. Zepf, M. Borghesi, and M. Geissler, Stable GeV Ion-Beam Acceleration from Thin Foils by Circularly Polarized Laser Pulses, Phys. Rev. Lett. **102**, 145002 (2009).

[32] A. Macchi, S. Veghini, and F. Pegoraro, "Light Sail" Acceleration Reexamined, Phys. Rev. Lett. **103**, 085003 (2009).

[33] B. Qiao, M. Zepf, M. Borghesi, B. Dromey, M. Geissler, A. Karmakar and P. Gibbon, Radiation-Pressure Acceleration of Ion Beams from Nanofoil Targets: The Leaky Light-Sail Regime, Phys. Rev. Lett. **105**, 155002 (2010).

[34] X. F. Shen, B. Qiao, A. Pukhov, S. Kar, S. P. Zhu, M. Borghesi, and X. T. He, Scaling laws for laser-driven ion acceleration from nanometer-scale ultrathin foils, Phys. Rev. E **104**, 025210 (2021).

[35] F. Pegoraro and S. V. Bulanov, Photon Bubbles and Ion Acceleration in a Plasma Dominated by the Radiation Pressure of an Electromagnetic Pulse, Phys. Rev. Lett. **99**, 065002 (2007).

[36] C. A. J. Palmer, J. Schreiber, S. R. Nagel, N. P. Dover, C. Bellei, F. N. Beg, S. Bott, R. J. Clarke, A. E. Dangor, S. M. Hassan *et al.*, Rayleigh-Taylor Instability of an Ultrathin Foil Accelerated by the Radiation Pressure of an Intense Laser, Phys. Rev. Lett. **108**, 225002 (2012).

[37] S. C. Wilks, A. B. Langdon, T. E. Cowan, M. Roth, M. Singh, S. Hatchett, M. H. Key, D. Pennington, A. MacKinnon, and R. A. Snavely, Energetic proton generation in ultra-intense laser-solid interactions, Phys. Plasmas **8**, 542 (2001).

[38] P. Mora, Thin-foil expansion into a vacuum, Phys. Rev. E **72**, 056401 (2005).

[39] A. Alejo, H. Ahmed, A. G. Krygier, R. Clarke, R. R. Freeman, J. Fuchs, A. Green, J. S. Green, D. Jung, A. Kleinschmidt *et al.*, Stabilized Radiation Pressure Acceleration and Neutron Generation in Ultrathin Deuterated Foils, Phys. Rev. Lett. **129**, 114801 (2022).

[40] Y. Wan, I. A. Andriyash, W. Lu, W. B. Mori, and V. Malka, Effects of the Transverse Instability and Wave Breaking on the Laser-Driven Thin Foil Acceleration, Phys. Rev. Lett. **125**, 104801 (2020).

[41] T. D. Arber, K. Bennett, C. S. Brady, A. Lawrence-Douglas, M. G. Ramsay, N. J. Sircombe, P. Gillies, R. G. Evans, H. Schmitz, A. R. Bell *et al.*, Contemporary particle-in-cell approach to laser-plasma modelling, Plasma Phys. Controlled Fusion **57**, 113001 (2015).

[42] X. Q. Yan, C. Lin, Z. M. Sheng, Z. Y. Guo, B. C. Liu, Y. R. Lu, J. X. Fang, and J. E. Chen, Generating High-Current Monoenergetic Proton Beams by a Circularly Polarized Laser Pulse in the Phase-Stable Acceleration Regime, Phys. Rev. Lett. **100**, 135003 (2008).

[43] T. P. Yu, A. Pukhov, G. Shvets, and M. Chen, Stable Laser-Driven Proton Beam Acceleration from a Two-Ion-Species Ultrathin Foil, Phys. Rev. Lett. **105**, 065002 (2010).

[44] H. Daido, M. Nishiuchi, and A. S. Pirozhkov, Review of laser-driven ion sources and their applications, Rep. Prog. Phys. **75**, 056401 (2012).

[45] T. E. Cowan, J. Fuchs, H. Ruhl, A. Kemp, P. Audebert, M. Roth, R. Stephens, I. Barton, A. Blazevic, E. Brambrink *et al.*, Ultralow Emittance, Multi-MeV Proton Beams from a Laser Virtual-Cathode Plasma Accelerator, Phys. Rev. Lett. **92**, 204801 (2004).

[46] S. A. Narod, J. Iqbal, A. Jakubowska, T. Huzarski, P. Sun, C. Cybulski, J. Gronwald, T. Byrski and J. Lubinski, Are two-centimeter breast cancers large or small? Curr. Oncol. **20**, 205 (2013).

[47] S. Rieken, D. Habermehl, T. Haberer, O. Jaekel, J. Debus, and S. E. Combs, Proton and carbon ion radiotherapy for primary brain tumors delivered with active raster scanning at the Heidelberg Ion Therapy Center (HIT): Early treatment results and study concepts, Radiat. Oncol. **7**, 41 (2012).

[48] S. Agostinelli, J. Allison, K. Amako, J. Apostolakis, H. Araujo, P. Arce, M. Asai, D. Axen, S. Banerjee, G. Barrand *et al.*, GEANT4—a simulation toolkit, Nucl. Instrum. Methods Phys. Res., Sect. A **506**, 250 (2003).

[49] W. T. Chu, J. W. Staples, B. A. Ludewigt, T. R. Renner, R. P. Singh, M. A. Nyman, J. M. Collier, I. K. Daftari, P. L. Petti, J. R. Alonso *et al.*, Performance specifications for proton medical facility, Report No. 33749, Lawrence Berkeley Laboratory, 1993 (unpublished), DOI:10.2172/10163935.

[50] F.-E. Brack, F. Kroll, L. Gaus, C. Bernert, E. Beyreuther, T. E. Cowan, L. Karsch, S. Kraft, L. A. Kunz-Schughart, E. Lessmann *et al.*, Spectral and spatial shaping of laser-driven proton beams using a pulsed high-field magnet beamline, Sci. Rep. **10**, 9118 (2020).

[51] H. Iwata, M. Murakami, Y. Demizu, D. Miyawaki, K. Terashima, Y. Niwa, M. Mima, T. Akagi, Y. Hishikawa, and Y. Shibamoto, High-dose proton therapy and carbon-ion therapy for stage I nonsmall cell lung cancer, Cancer **116**, 2476 (2010).

[52] E. J. Hall, Radiation dose-rate: A factor of importance in radiobiology and radiotherapy, Brit. J. Radiol. **45**, 81 (1972).

[53] C. N. Danson, C. Haefner, J. Bromage, T. Butcher, J.-C. F. Chanteloup, E. A. Chowdhury, A. Galvanauskas, L. A. Gizzi, J. Hein *et al.*, Petawatt and exawatt class lasers worldwide, High Power Laser Sci. Eng. **7**, e54 (2019).